



#### OPEN ACCESS

EDITED BY  
Chamindra L Vithana,  
Southern Cross University, Australia

REVIEWED BY  
Fasih Ullah Haider,  
Chinese Academy of Sciences (CAS),  
China  
Martin Lukac,  
University of Reading, United Kingdom  
Fabiano Simplicio Bezerra,  
Federal Rural University of Pernambuco,  
Brazil

\*CORRESPONDENCE  
Peter Onyisi Uhuegbue,  
✉ peter.uhuegbue@zalf.de

RECEIVED 27 October 2025  
REVISED 03 February 2026  
ACCEPTED 17 February 2026  
PUBLISHED 04 March 2026

CITATION  
Uhuegbue PO, Hoffmann M, Lück M,  
Grahmann K, Kalbitz K and Schaller J  
(2026) Effects of amorphous silica on CO<sub>2</sub>  
and N<sub>2</sub>O emissions mediated by water-  
filled pore space in diverse  
agricultural soils.  
*Front. Environ. Sci.* 14:1733653.  
doi: 10.3389/fenvs.2026.1733653

COPYRIGHT  
© 2026 Uhuegbue, Hoffmann, Lück,  
Grahmann, Kalbitz and Schaller. This is an  
open-access article distributed under the  
terms of the [Creative Commons  
Attribution License \(CC BY\)](https://creativecommons.org/licenses/by/4.0/). The use,  
distribution or reproduction in other  
forums is permitted, provided the original  
author(s) and the copyright owner(s) are  
credited and that the original publication  
in this journal is cited, in accordance with  
accepted academic practice. No use,  
distribution or reproduction is permitted  
which does not comply with these terms.

# Effects of amorphous silica on CO<sub>2</sub> and N<sub>2</sub>O emissions mediated by water-filled pore space in diverse agricultural soils

Peter Onyisi Uhuegbue<sup>1,2\*</sup>, Mathias Hoffmann<sup>3</sup>, Matthias Lück<sup>3</sup>,  
Kathrin Grahmann<sup>4</sup>, Karsten Kalbitz<sup>2</sup> and Jörg Schaller<sup>1,5</sup>

<sup>1</sup>Leibniz Center for Agricultural Landscape Research (ZALF), working group for Agricultural Biogeochemistry, Müncheberg, Germany, <sup>2</sup>Technische Universität Dresden Soil Resources and Land Use, Institute of Soil Science and Site Ecology, Tharandt, Germany, <sup>3</sup>Leibniz Center for Agricultural Landscape Research (ZALF), working group for change to Ecophysiology of Water and Matter Cycling, Müncheberg, Germany, <sup>4</sup>Leibniz Centre for Agricultural Landscape Research (ZALF), working group for Resource-Efficient Cropping Systems, Müncheberg, Germany, <sup>5</sup>University of Gießen, FB 09 Agrarwissenschaften, Ökotrophologie und Umweltmanagement, Gießen, Germany

**Introduction:** Silicon (Si) is abundant in the Earth's crust; however, its amorphous form (ASi) is often depleted in agricultural soils due to crop uptake and removal with harvest. While ASi benefits plant nutrient uptake and growth, its effects on soil pore characteristics, such as water-filled pore space (WFPS), and regulating greenhouse gas (GHG) emissions remain poorly understood.

**Methods:** We investigated the effect of ASi addition on soil bulk density, WFPS, and subsequent N<sub>2</sub>O and CO<sub>2</sub> emission dynamics in two soil types of differing texture: Luvisols (modest silt and clay) and Arenosols (low silt and clay). In a first experiment (Experiment I), soils were amended with 0% (control), 1%, 5%, and 10% ASi (w/w, relative to soil dry weight) to assess effects on bulk density and WFPS under fixed water input. A second experiment (Experiment II) investigated the effect of 0% (control) and 1% ASi (w/w, relative to soil dry weight) on N<sub>2</sub>O and CO<sub>2</sub> emissions.

**Results:** The addition of ASi altered soil bulk density, leading to a decrease in WFPS. This was in particular the case at 10% ASi addition to Luvisols. In Arenosols, WFPS first increased at 1% ASi before finally declining at higher rates as well. In experiment II, 1% ASi addition reduced CO<sub>2</sub> emissions in Arenosols by ~42–45% and N<sub>2</sub>O by 8%–44%, but increased CO<sub>2</sub> in Luvisol by ~47% and N<sub>2</sub>O emissions by ~18–57%.

**Discussion:** The contrasting responses were texture-dependent, with ASi affecting soil physical properties and associated N<sub>2</sub>O and CO<sub>2</sub> emissions differently in Luvisols and Arenosols, consistent with inferred effects on pore structure and water retention. As these results are derived from controlled incubation conditions using disturbed soil cores under constant temperature and fixed water input, further field-based investigations are needed to assess the *in-situ* effects of a broader applicability of ASi.

#### KEYWORDS

amorphous silica, arenosol, bulk density, greenhouse gas emissions, luvisol, silicon, water-filled-pore space

# 1 Introduction

Silicon (Si), the second most abundant element in the earth's crust, occurs in many minerals (Wedepohl, 1995; Ma and Yamaji, 2006; Schaller et al., 2021). Soil Si occurs as dissolved silicic acid, adsorbed Si, amorphous silica (ASi, including biogenic ASi such as phytoliths and diatom shells), and Si bound in primary and secondary silicate minerals (Schaller et al., 2021; Bezerra et al., 2025).

However, the amorphous silica (ASi) concentration in agricultural soils is often depleted, typically falling below 1%, and in many cases approaching 0% (Schaller et al., 2021; Schaller et al., 2025). The depletion of ASi in agricultural soils occurs because most crops accumulate Si, at crop-specific rates, with high Si accumulators including grasses and cereals (e.g., rice, wheat, maize, and sugarcane), medium accumulators including some legumes (e.g., soybeans), while many dicotyledonous crops, including most vegetables, tuber crops (e.g., potato), and oilseed crops (e.g., rapeseed, sunflower), are low Si accumulators (Guntzer et al., 2012; Rea et al., 2022), resulting in the removal of large amounts of Si from the field through crop harvest (Struyf et al., 2010; Schaller et al., 2021). At the same time, unlike essential nutrients, Si is rarely replenished through fertilization, leading to a progressive decline in soil Si contents, although recent field studies demonstrate that amorphous silica can be applied at field scale using naturally occurring materials such as diatomaceous earth (Madegwa et al., 2025; Schaller et al., 2025). Despite not being classified as an essential plant nutrient (Fertilizer and Service; (Mengel and Kirkby, 1987)), Si has been shown to affect soil properties, improve nutrient uptake, and thus enhance plant resilience against biotic and abiotic stresses (Pati et al., 2016; Galindo et al., 2021; Martos-García et al., 2025). For instance, it has been reported that ASi changes soil physical properties, such as bulk density or porosity, as well as water retention, where the extent of change depends on the initial soil texture (Barbosa et al., 2024). Moreover, studies found that ASi addition to soil, improved N uptake in young rice, olive, maize, as well as wheat plants, leading to increased growth and yield (Pati et al., 2016; Galindo et al., 2021; Martos-García et al., 2025). Similarly, Hoffmann et al. (2025) showed that ASi enhanced plant nitrogen uptake, potentially limiting nitrogen availability for microbial processes like nitrification and denitrification, which in turn led to a roughly 30% reduction in N<sub>2</sub>O emissions. Additionally, ASi has been associated with higher soil CO<sub>2</sub> emissions (Hoffmann et al., 2025). This increase has been linked to enhanced biomass production and associated microbial and root respiration as a proposed mechanism, potentially resulting from ASi-induced increases in carbon inputs to the soil through root exudates and organic matter decomposition (Hoffmann et al., 2025). However, while previous studies have mainly been focused on the role of ASi in plant nutrition, stress tolerance, and the modification of soil physical properties, direct mechanistic links between ASi-induced changes in bulk density and WFPS and the resulting CO<sub>2</sub> and N<sub>2</sub>O emissions under a controlled, standardized water input across contrasting soil textures remain poorly quantified.

ASi has a lower bulk density (0.056–0.230 g cm<sup>-3</sup>) (Liu et al., 2003) than most mineral soils (1.3–1.8 g cm<sup>-3</sup>) (Sagona et al., 2016). Its addition can thus reduce soil bulk density, thereby altering water-filled-pore space (WFPS). Changes in these properties can significantly impact GHG emissions by modifying microbial

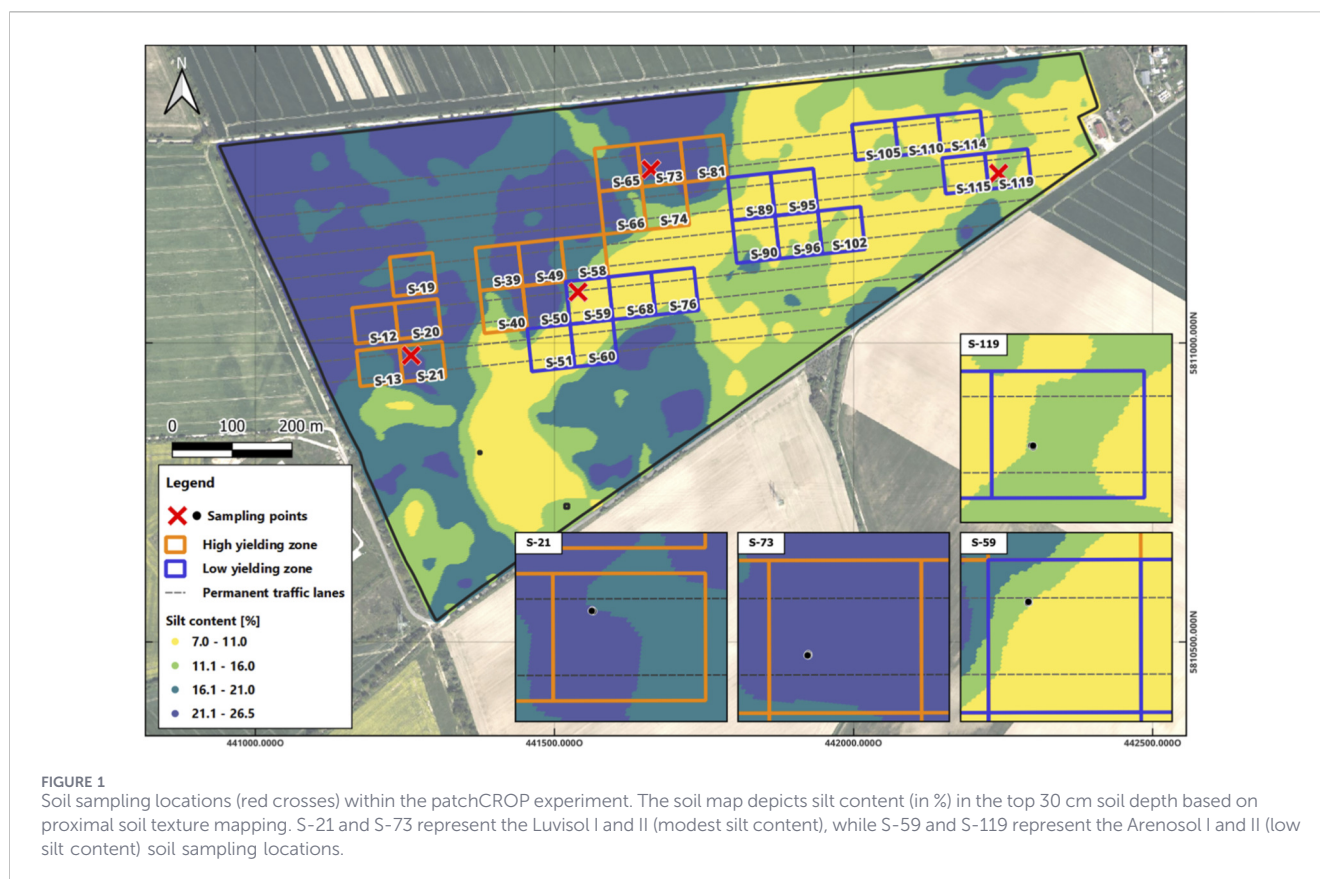
activity and gas diffusion in soils. For instance, a reduction in bulk density may improve soil aeration, potentially influencing N<sub>2</sub>O and CO<sub>2</sub> flux dynamics.

Barbosa et al. (2024) found that ASi improved aggregate stability and modified pore size distribution, increasing meso- and micropore volume in coarse-textured soils, while no such effect was observed in finer-textured soils. While this change in pore structure enhances moisture retention, particularly in coarse-textured soils (Zarebanadkouki et al., 2022), it may also affect soil aeration, thereby lowering WFPS compared to soil without ASi under identical water input.

As WFPS regulates the balance between aerobic and anaerobic conditions (Linn and Doran, 1984; Butterbach-Bahl et al., 2013), changes in WFPS due to ASi can substantially impact N<sub>2</sub>O and CO<sub>2</sub> emissions. In well-aerated soils, CO<sub>2</sub> emissions typically peak around 60% WFPS, where microbial respiration is optimized, and decline at lower (<60%) or higher (>60%) WFPS due to oxygen or water limitation (Linn and Doran, 1984). For N<sub>2</sub>O, different microbial processes may dominate across varying WFPS. Nitrification also has its optimum around 60% WFPS but produces a relatively small amount of N<sub>2</sub>O. With higher WFPS (80%–100%), a decrease in oxygen availability favors denitrification (the dominant pathway for N<sub>2</sub>O production), resulting in higher N<sub>2</sub>O emissions (Linn and Doran, 1984; Davidson and Verchot, 2000). However, above 80% WFPS, increased oxygen depletion might also result in complete denitrification, converting N<sub>2</sub>O to N<sub>2</sub> (Davidson and Verchot, 2000; Wu et al., 2017). At the same time, isotopic and microscale studies show that denitrification can already occur at about 60% WFPS, and both nitrification and denitrification may co-occur within aggregates due to microsite oxygen limitation (Müller and Clough, 2014; Wrage-Mönnig et al., 2018; Schlüter et al., 2025). In contrast to N<sub>2</sub>O and CO<sub>2</sub>, methane (CH<sub>4</sub>) plays a minor role in well-aerated agricultural soils, which typically act as a net sink for atmospheric CH<sub>4</sub> due to microbial methane oxidation (Hansen et al., 2024). Changes in soil physical properties and aeration induced by ASi addition could therefore potentially enhance CH<sub>4</sub> uptake in the upper soil layers, although CH<sub>4</sub> fluxes are expected to remain small compared to N<sub>2</sub>O and CO<sub>2</sub>. In addition to oxygen dynamics, N<sub>2</sub>O formation depends strongly on carbon and nitrate availability and specific microbes (Davidson et al., 2000); in coarse-textured soils with low soil organic carbon (SOC), limited availability of organic carbon and nitrate can constrain rates and alter typical WFPS emission patterns, as well as N<sub>2</sub>O: N<sub>2</sub> ratios.

Given the strong impact of WFPS, aeration, and nitrogen availability on microbial processes and GHG emissions, understanding the actual effect of ASi addition is critical, especially in the case of texture-diverse agricultural soils where responses might differ. However, it is still not certain whether ASi shifts bulk density and pore water status in the same direction in coarse-versus fine-textured soils, and how such shifts correspond to CO<sub>2</sub> and N<sub>2</sub>O emissions. For example, Maillet et al. (2025) demonstrated that soils with lower meso- and macroporosity exhibited higher WFPS and greater N<sub>2</sub>O emission, underlying the critical role of pore connectivity and size distribution in regulating gas exchange and microbial processes.

Hence, this study aims to investigate how ASi addition affects soil bulk density, WFPS, and the emission of key GHGs, particularly



$N_2O$  and  $CO_2$ , which are most relevant in mineral and agricultural soils. We hypothesize that (i) under equivalent water input, ASI addition to soil changes the soil bulk density and thereby alters WFPS compared to soils without ASI addition (Experiment I) and ii) these ASI-induced shifts in bulk density and WFPS will be associated with changes in  $CO_2$  and  $N_2O$  emissions during incubation (Experiment II). However, the magnitude and direction of these changes may depend on the soil's texture. To test these hypotheses, two experiments (Experiment I and II) were performed using two different soil types varying in their silt and clay content: Luvisol (modest silt and clay content), which refers to intermediate clay fractions of ~15–20% relative to other studied soils, and Arenosol (low silt and clay content). In experiment I, soils were treated without (controls) and with different amounts of ASI (w/w relative to soil dry weight) to determine its effect on soil bulk density and WFPS. Here, higher ASI rates were used to resolve influences soil bulk density and the derived WFPS across a broader addition range. In experiment II, soils amended with 1% ASI and unamended (controls) were incubated to determine ASI's impact on soil  $N_2O$  and  $CO_2$  emissions. We used 1% ASI (relative to soil dry weight) in the incubation experiment (Experiment II) because this level is within the range of ASI contents typically found in non-agricultural soils (~1.2% on average) and is higher than what is often observed in cultivated soils, where ASI is frequently depleted to <1% in majority zero (Schaller et al., 2025). Bulk density and WFPS in Experiment II were inferred from the standardized packing and water addition procedures, based on the responses quantified in Experiment I. By addressing the impact of ASI addition on bulk density, WFPS, and finally  $N_2O$  and  $CO_2$  emissions, we seek to

provide new insights into the potential of ASI-based soil amendments as a measure to modify soil physical conditions and thereby contribute to the mitigation of agricultural  $N_2O$  and  $CO_2$  emissions, depending on soil texture and management.

## 2 Materials and methods

### 2.1 Sampling site

For this study, we collected four soil samples within the patchCROP experiment (Figure 1; (Grahmann et al., 2024); at Tempelberg, Germany (52°26'37"N 14°09'39"E). The experimental field covers a total area of 70 ha and features an average annual air temperature of 9.6 °C and annual precipitation of 472 mm (ZALF climate station). Its soil mostly comprises high sandy glacial till derived from ground moraine material, with modest variations in silt and clay content. Sampling was designed to capture this textural continuum within the experimental field. Accordingly, the four sampling locations were specifically chosen for their predominantly sandy texture and represent variations in silt and clay content of the two dominant soil types present at the site, namely, Luvisol with modest silt and clay content and Arenosol with low silt and clay content, as classified according to the World Reference Base (Grahmann et al., 2024). The focus on sandy soils was motivated by previous findings showing that the effects of ASI are most pronounced in such soils, particularly in enhancing soil moisture levels (Zarebanadkouki et al., 2024). Soil samples from each of the four sampling locations were taken as a mixed topsoil

**TABLE 1** Summary of soil physicochemical properties and CO<sub>2</sub> and N<sub>2</sub>O fluxes under different ASi treatments at four sampling locations (Luvisol I and II, Arenosol I and II). Reported are total cumulative CO<sub>2</sub> and N<sub>2</sub>O fluxes (mean ± SD, n = 4), mineral nitrogen content (N<sub>min</sub>; mean ± SD, n = 4) assessed at 1% ASi (Experiment II), bulk density (g cm<sup>-3</sup>; mean ± SD, n = 3), and water-filled pore space (WFPS; mean ± SD, n = 3) determined across all ASi rate (Experiment I). Soil texture is given as sand, silt, and clay contents (determined across all ASi rate), and total nitrogen TN and total organic carbon content (TOC) are provided for each sampling location. TN and TOC refer to untreated soils only. For bulk density and WFPS, statistical comparisons were made between each ASi treatment and its respective control using a *post hoc* test, while a permutation test was applied for CO<sub>2</sub> and N<sub>2</sub>O to determine the difference between 1% ASi treatment and the respective control treatments. Treatments showing significant differences (p-value < 0.05) are indicated using different superscript letters.

Sampling location	Treatment	CO <sub>2</sub> flux	N <sub>2</sub> O flux	NH <sub>4</sub> <sup>-</sup> N <sub>KCl</sub>	NO <sub>3</sub> <sup>-</sup> N <sub>KCl</sub>	Bulk density	WFPS	Sand	Silt	Clay	TOC	TN
		mg CO <sub>2</sub> -C g <sup>-1</sup> (n = 4)	μg N <sub>2</sub> O-N g <sup>-1</sup> (n = 4)	mg 100 g <sup>-1</sup> (n = 4)	mg 100 g <sup>-1</sup> (n = 4)	g cm <sup>-3</sup> (n = 3)	% (n = 3)			%		
Luvisol I	Control	33.6 <sup>a</sup> ± 12.8	3.1 <sup>a</sup> ± 1.3	0.2 ± 0.1	1.9 ± 0.8	1.6 <sup>a</sup> ± 0.0	66 <sup>a</sup> ± 2.6	74	25	2	0.9	0.1
	ASi - 1%	49.3 <sup>b</sup> ± 2.6	4.9 <sup>a</sup> ± 0.8	0.1 ± 0.0	2.3 ± 0.2	1.5 <sup>a</sup> ± 0.0	63 <sup>a</sup> ± 2.8	71	26	4	-	-
	ASi - 5%	-	-	-	-	1.4 <sup>b</sup> ± 0.0	52 <sup>b</sup> ± 2.5	68	26	5	-	-
	ASi - 10%	-	-	-	-	0.5 <sup>c</sup> ± 0.0	11 <sup>c</sup> ± 0.8	67	27	6	-	-
Luvisol II	Control	28.8 <sup>a</sup> ± 2.7	4.3 <sup>a</sup> ± 3.4	0.1 ± 0.0	4.9 ± 0.2	1.7 <sup>a</sup> ± 0.0	65 <sup>a</sup> ± 0.7	74	22	4	1.2	0.1
	ASi - 1%	45.5 <sup>a</sup> ± 31.7	5.2 <sup>a</sup> ± 3.9	0.1 ± 0.0	4.6 ± 0.1	1.5 <sup>a</sup> ± 0.0	59 <sup>a</sup> ± 3.8	74	22	4	-	-
	ASi - 5%	-	-	-	-	1.4 <sup>b</sup> ± 0.0	48 <sup>b</sup> ± 2.5	70	25	5	-	-
	ASi - 10%	-	-	-	-	0.6 <sup>b</sup> ± 0.0	12 <sup>c</sup> ± 0.8	69	25	6	-	-
Arenosol I	Control	68.1 <sup>a</sup> ± 16.4	3.9 <sup>a</sup> ± 1.5	0.1 ± 0.0	0.7 ± 0.6	1.5 <sup>a</sup> ± 0.0	68 <sup>a</sup> ± 3.5	86	12	2	0.7	0.1
	ASi - 1%	37.4 <sup>b</sup> ± 8.5	2.2 <sup>b</sup> ± 0.2	0.3 ± 0.3	0.9 ± 0.8	1.6 <sup>a</sup> ± 0.0	71 <sup>a</sup> ± 3.0	81	16	3	-	-
	ASi - 5%	-	-	-	-	1.6 <sup>a</sup> ± 0.6	66 <sup>a</sup> ± 4.6	79	19	5	-	-
	ASi - 10%	-	-	-	-	0.6 <sup>b</sup> ± 0.7	12 <sup>b</sup> ± 1.6	74	19	6	-	-
Arenosol II	Control	44.3 <sup>a</sup> ± 18.5	5.8 <sup>a</sup> ± 3.6	0.1 ± 0.0	3.0 ± 0.2	1.7 <sup>a</sup> ± 0.0	82 <sup>a</sup> ± 5.3	88	11	1	0.9	0.1
	ASi - 1%	25.5 <sup>b</sup> ± 2.5	5.3 <sup>a</sup> ± 4.7	0.1 ± 0.0	3.1 ± 0.1	1.8 <sup>a</sup> ± 0.2	95 <sup>b</sup> ± 4.3	87	12	1	-	-
	ASi - 5%	-	-	-	-	1.6 <sup>b</sup> ± 0.6	63 <sup>c</sup> ± 5.2	81	12	6	-	-
	ASi - 10%	-	-	-	-	0.6 <sup>c</sup> ± 0.1	12 <sup>d</sup> ± 2.6	78	13	9	-	-

The superscript letters [a, b, c, d] indicate statistically significant differences among treatments. Treatments that do not share a common superscript letter are significantly different at p-value < 0.05.

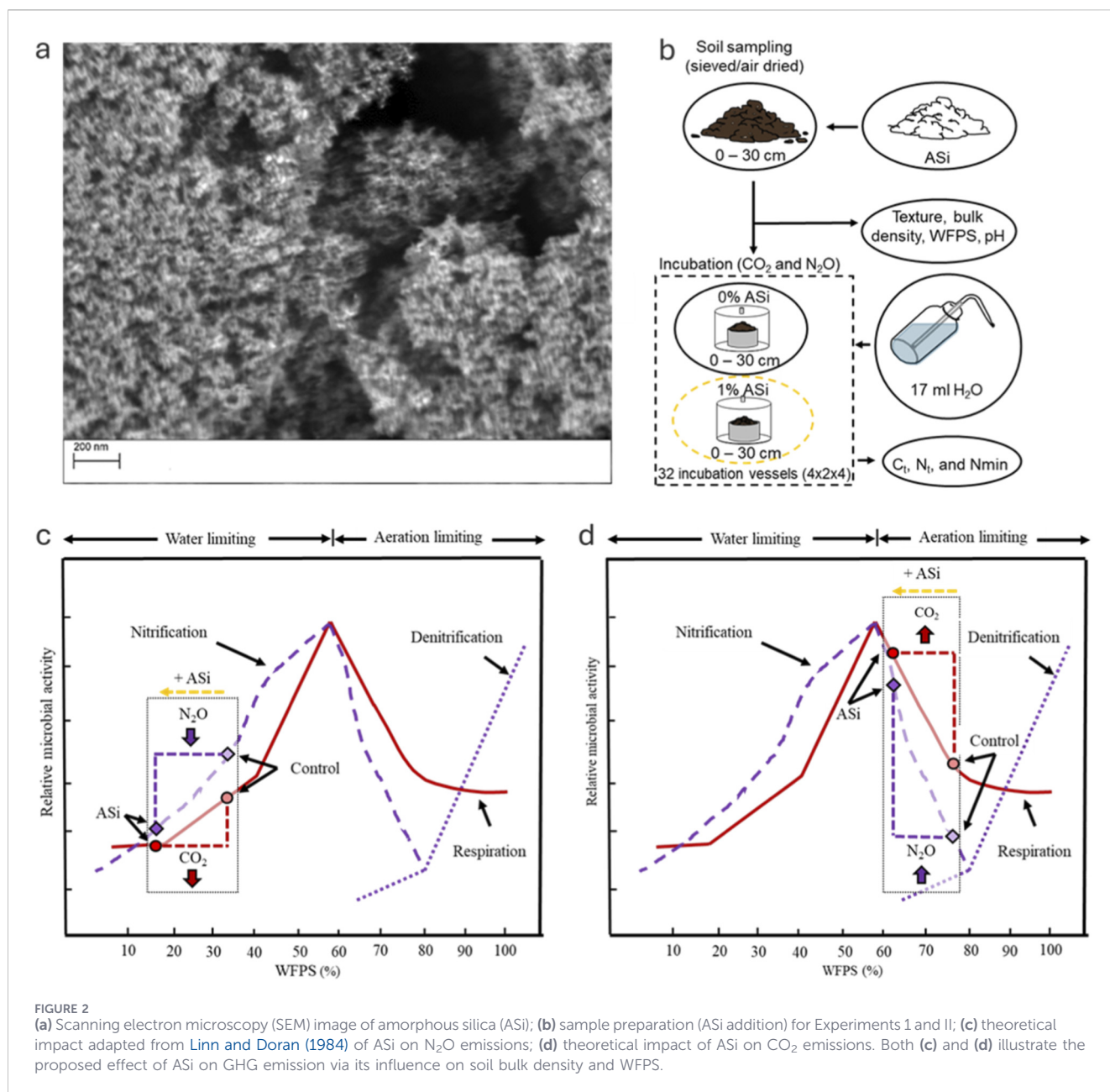
(0–30 cm) sample (n = 3) using an auger. After sampling, composite samples of each location were oven-dried at 40 °C, sieved through a 2 mm mesh, and homogenized for subsequent experiments and analyses, including water holding capacity (WHC), WFPS determination, and incubation setup.

## 2.2 Soil physical and chemical characterization

The WHC was determined using Luvisol I, selected due to its modestly finer texture relative to other studied soils (Table 1) with expected higher WHC, and was used as a reference to define a standardized water addition applied to all soils. This approach ensures identical absolute water input across soils, isolating ASi-induced changes in bulk density and WFPS. Using a single reference soil is reasonable in this context because all soils originate from the

same field and, under natural conditions, would receive the same rainfall. Nevertheless, because WHC differs among textures, true % WHC and absolute WFPS still differ among soils, representing a methodological limitation. Future studies could determine WHC individually for each soil to directly link ASi-induced physical changes to soil water status. For this, 100 g of air-dried Luvisol I (in three replicates) was weighed into a steel core (250 cm<sup>3</sup> volume) with one of the ends of the core covered with a perforated material that allows water drainage. About 60 mL of water was added to the soil samples, and afterward, the soil samples were allowed to drain for 24 h at a temperature of 22 °C. The WHC of the soil was then calculated by taking the difference in the weight of the soil before the addition of water and the final weight after allowing the water to drain for 24 h.

The soil texture analysis was performed using a hydrometer, following a modified Bouyoucos method (Beretta et al., 2014).



Briefly, 50 g of dry soil (three replicates per plot) was dispersed in 100 mL of 25% sodium hexametaphosphate (technical Calgon, Bioquim, Montevideo, Uruguay) for 16 h on a reciprocating shaker. The suspension was then mixed for 5 minutes using an electric mixer in a Bouyoucos blender cup. After transferring to a 2 L sedimentation cylinder, deionized water was added up to the 2 L mark, and the mixture was manually agitated. The first hydrometer reading, taken after 40 s, determined sand content, while the second reading, recorded after 2 hours, estimated clay content. The silt fraction was calculated as the difference between the sand and clay values. Measurements were performed at 20 °C–22 °C, with temperature corrections applied when necessary.

Mineral nitrogen (N<sub>min</sub>; sum of NH<sub>4</sub><sup>+</sup> and NO<sub>3</sub><sup>-</sup>) was determined for both the initial soil samples and soils with and without 1% ASi after incubation (experiment II). For the extraction,

80 mL of 1 M potassium chloride (KCl) solution was added to 20 g of soil in 100 mL extraction tubes. Afterward, the mixture was shaken for 60 min at ~20 °C. After 30 min of shaking, it was filtered using a MACHERY-NAGEL MN 619 1/4 G filter paper (Keeney and Nelson, 1982). Ammonium (NH<sub>4</sub><sup>+</sup>) analysis based on the Bertholet reaction (Weatherburn, 1967) was determined by mixing 5 mL of the filtrate with Bertholet reagent and was allowed to react for 30 min, before measuring the absorbance at 660 nm. For nitrate determination, another 5 mL of the filtrate was treated with a cadmium reduction column to convert NO<sub>3</sub><sup>-</sup> to NO<sub>2</sub><sup>-</sup>, after which the sample was then mixed with Griess reagent and was allowed to react for 20 min before measuring at 540 nm. Both NH<sub>4</sub><sup>+</sup> and NO<sub>3</sub><sup>-</sup> were measured spectrophotometrically (Gallery Plus; ThermoFisher SCIENTIFIC GmbH). The total concentration of organic carbon (TOC) and total nitrogen (TN) of the original

soil samples was analyzed using a TOC analyzer (TNM-L, Shimadzu, Japan).

### 2.3 Experiment I: determination of the effect of ASi on bulk density and WFPS

Figure 2 illustrates how ASi addition, through alteration of bulk density and thus WFPS, might affect N<sub>2</sub>O and CO<sub>2</sub> emissions as a result of the theoretical relationship between WFPS and microbial activity, adapted from Linn and Doran (1984). The ASi used in this study was pyrogenic silica (Aerosil 300, Evonik, Germany) with a BET specific surface area of 300 m<sup>2</sup> g<sup>-1</sup> and a particle size between 7 and 15 nm (Evonik-Industries, 2018), shown in the SEM image in Figure 2a. The addition of ASi (Figure 2a) may reduce bulk density (Figure 2b) and enhance water-holding capacity, thereby lowering WFPS compared to soil without ASi addition. This shift in WFPS, in turn, could modify N<sub>2</sub>O and CO<sub>2</sub> emissions (Figures 2c,d) depending on the amount of available water, potentially altering the balance between nitrification, denitrification, and microbial respiration.

To determine the actual effect of ASi addition on soil bulk density and WFPS, 50 g of air-dried soil from each sampling location was mixed with ASi at application rates of 0% (control), 1%, 5%, and 10% (w/w relative to soil dry weight). Each application rate was replicated three times (n = 3). We use Aerosil, pyrogenic ASi, because its physicochemical properties are comparable to those of biogenic ASi (Belton et al., 2012). Soil-ASi mixtures were prepared by placing the required amounts of dry soil and ASi into 16 individual containers per run and homogenizing them on an end-over-end shaker for 24 h to ensure uniform distribution of ASi throughout the soil. Each mixture was then transferred into a soil steel core (250 cm<sup>3</sup> volume) in small increments, gently tapping the core after each addition to achieve uniform compaction. The resulting packing represented typical field bulk density values for these soil types (Engels et al., 2025), supporting the suitability of the approach for examining treatment effects. The final volume of each soil-ASi mixture in the core was measured, and subsequently, bulk density was determined based on the mass of the air-dry soils. To obtain a potential change in WFPS, 8.5 mL of water (i.e., 60% of WHC of Luvisol I—reference soil, which means slightly different WFPS for the four soils) was added to each of the soil-ASi mixtures. This fixed water input produced slightly different WFPS values among soils due to texture and bulk density differences. Initial soil moisture was not measured because soils were oven-dried prior to ASi amendment and water addition. Therefore, WFPS values were calculated (using Equation 1) solely from the added water volume under standardized water addition derived from Luvisol I as reference. As a result, WFPS represents approximate values and is used here as a comparative index based on added water under a standardized setup, rather than an absolute value or exact field equivalent moisture conditions.

$$\%WFPS = \left( \frac{\theta_v}{TP} \right) \times 100 \quad (1)$$

where  $\theta_v$  is the volumetric water content (%), TP is the total pore space calculated as  $(I - \frac{P_b}{P_p}) \times 100$  where  $P_b$  is the soil bulk density (g cm<sup>-3</sup>) and  $P_p$  is the particle density (~2.65 g cm<sup>-3</sup>).

### 2.4 Experiment II: determination of the effect of ASi on CO<sub>2</sub> and N<sub>2</sub>O emissions

To assess the effect of ASi addition on CO<sub>2</sub> and N<sub>2</sub>O emissions, we incubated 100 g of soil from each of the four sampling locations for 14 consecutive days, with and without 1% ASi addition. The 1% ASi treatment was chosen because agricultural soils are typically depleted by ~1% ASi compared to natural soils, and a difference of 1% ASi is also known to alter soil moisture levels (Schaller et al., 2020; Schaller et al., 2021). Right before incubation, 17 mL of water (equivalent to 60% of WHC) was added to each of the 100 g soil samples with and without ASi mixed in. This water addition was equivalent to 8.5 mL applied to 50 g of soil during the bulk density and WFPS assessment in Experiment I. While we use 100 g of soil in a fixed volume vessel (13 cm in diameter and height) in the incubation experiment (Experiment II). Bulk density and volumetric water content were not measured or adjusted in the incubation vessels (comparable density to Experiment I is inferred from standardized filling procedure); therefore, physical conditions during gas flux measurements are inferred from standardized packing and fixed water addition. The soil-ASi mixtures were filled into the incubation vessels (13 cm in diameter and height) to a fixed volume, ensuring the same headspace among samples. Packing was done by gently tapping the vessel walls to achieve a uniform density comparable to that measured in Experiment I. This ensured consistency in soil structure and porosity across treatments. Each treatment was replicated four times (n = 4). Soil CO<sub>2</sub> and N<sub>2</sub>O emissions were continuously measured using the soil incubation system described in detail by Rillig et al. (2021). The system operates in a flow-through steady-state mode (Livingston and Hutchinson, 1995). It consists of 16 airtight, cylindrical incubation vessels (13 cm in diameter and height), constructed from commercially available KG DN sewer pipes and accessories (Marley, Germany), and placed in a temperature-controlled (20 °C) box. Ambient air from a pressure vessel flows continuously through the headspace of the incubation vessels at 32 mL min<sup>-1</sup> to a gas analyzer (Picarro G2508; PICARRO, INC., Santa Clara, United States). A control channel allows ambient air to bypass the soil samples and flow directly from the pressure vessel to the gas analyzer at the same rate. To prevent soil samples within the incubation vessels from drying out over incubation time, the incoming air is humidified to 100% relative humidity before entering the incubation vessels. Gravimetric water content was not measured at the end of the incubation. Although inflow air was humidified to reduce drying, changes in soil water content over time cannot be excluded and may have influenced flux dynamics; however, we assumed WFPS remained approximately constant. N<sub>2</sub>O and CO<sub>2</sub> concentrations were measured at 1 Hz using a CRDS analyzer. Each incubation vessel was sequentially connected to the gas analyzer via a multiplexer, with one dedicated measurement channel per vessel and an additional control channel. Each channel was measured for 7 min per cycle. Air was continuously circulated between the incubation vessel headspace and the CRDS analyzer at a flow rate of 250 mL min<sup>-1</sup> using a low-leak diaphragm pump (A0702, Picarro, Santa Clara, CA, United States). The multiplexer directed air from each of the 17 channels (16 incubation vessels and one control channel) into the measurement circuit. Gas fluxes were calculated using the ideal gas law (Equation 2) based on measured CO<sub>2</sub> or N<sub>2</sub>O concentrations

in each channel and the equivalent concentrations in the control channel (Rillig et al., 2021):

$$F = \frac{\Delta C \cdot V \cdot \rho}{\Delta t \cdot A \cdot R \cdot (T + 273.15)} \quad (2)$$

where  $F$  is the flux rate ( $\mu\text{mol m}^{-2} \text{s}^{-1}$ ),  $\Delta C$  is the concentration difference between the incubation vessel outlet and the control channel ( $\text{mol mol}^{-1}$ ),  $V$  is the air flow rate into the headspace and the channels ( $\text{m}^3$ ),  $\rho$  is the atmospheric pressure (Pa),  $A$  is the chamber basal area ( $\text{m}^2$ ),  $\Delta t$  is the measurement time interval (s),  $R$  is the gas constant ( $8.314 \text{ m}^3 \text{ Pa K}^{-1} \text{ mol}^{-1}$ ), and  $T$  is the incubation temperature (K). Cumulative  $\text{N}_2\text{O}$  and  $\text{CO}_2$  fluxes over defined time intervals were calculated using a modified version of the modular R script described by (Hoffmann et al., 2015).

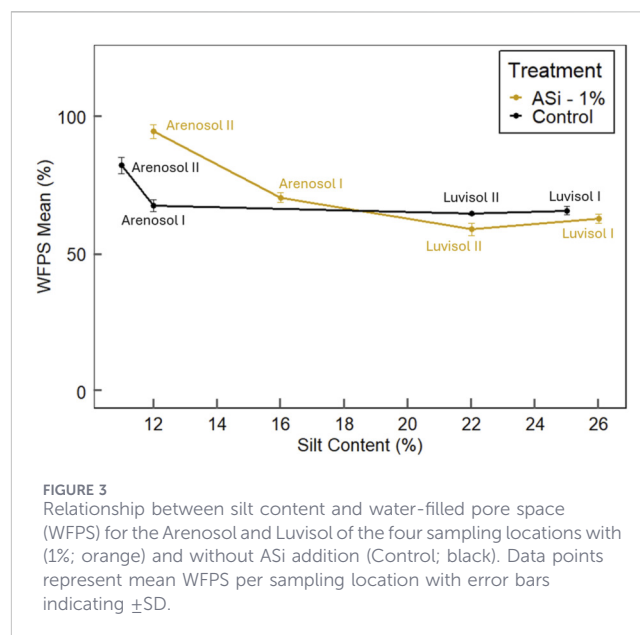
## 2.5 Statistical analysis and data visualization

Fluxes were calculated, and a visualization was made using the R computational environment, version 4.5.0 and R studio (R Core Team, 2013). The effects of ASi treatments, specifically control (0%), 1%, 5%, and 10% ASi on bulk density and WFPS across the two different soil types were assessed using a one-way analysis of variance (ANOVA). Given the sample size ( $n = 3$ , experiment I), the ANOVA assumptions were thoroughly examined to guarantee the validity of the analysis, particularly assessing the normality of residuals using the Shapiro-Wilk test. A Q-Q plot was used to further validate the results of the normality tests. A Levene's test was applied to evaluate the homogeneity of variance between the treatment groups. These diagnostic tests confirmed that the ANOVA assumptions and homogeneity of variance were satisfied, justifying the use of the parametric ANOVA approach. Following the ANOVA, a Tukey's *post hoc* test ( $p < 0.05$ ) was used to identify specific differences between treatment groups (control (0%), 1%, 5%, and 10% ASi) for the bulk density and WFPS (experiment I). Differences in measured  $\text{N}_2\text{O}$  and  $\text{CO}_2$  fluxes between control and 1% ASi treatments (Experiment II) were assessed using a two-sided exact permutation test ( $\alpha = 0.05$ ). The test statistic was the difference in group means (1% ASi vs. Control). The permutation distribution was generated by enumerating all possible treatment-label reallocations; with 4 replicates per treatment ( $n = 8$ ), this yield choose (8,4) = 70 permutations. Analyses were implemented in R (v4.5.0; RStudio) using base functionality (`utils:combn ()`) and standard base functions.

## 3 Results

### 3.1 Physicochemical soil properties

The studied soil varied in texture and organic carbon content (Table 1): Luvisols I and II were slightly finer (modest silt) and had higher TOC (~0.9–1.2%) than coarser Arenosols (sand-dominated) with lower TOC content (~0.7–0.9%). Across both soil types, increasing ASi addition (from 1% to 10%) shifted the particle size distribution towards finer fractions (high silt/clay and lower sand; Table 1). Total nitrogen (TN) content was similar for all studied soils of the four sampling locations, and  $\text{N}_{\text{min}}$  measured after



incubation did not differ significantly between control and 1% ASi addition or between soil types (Table 1).

### 3.2 Effect of ASi addition on bulk density and WFPS

Experiment showed that the addition of 1%, 5%, and 10% ASi altered soil bulk density and WFPS in both Arenosols and Luvisols. In Luvisol I and II, a non-significant decrease in bulk density due to 1% ASi addition compared to the control was found (Table 1), whereas bulk density decreased significantly at both 5% and 10% ASi addition compared to the control ( $p < 0.05$ ). In contrast, Arenosol I and II showed a non-significant increase in bulk density due to 1% ASi addition compared to the control treatment, followed by a decrease at 5% and 10% ASi addition. This decrease was significant for Arenosol I at both 5% and 10% ( $p < 0.05$ ) compared to the control, and for Arenosol II only at 10% ASi addition ( $p < 0.05$ ) compared to the control (Table 1). These changes in bulk density were accompanied by a change in calculated WFPS (Table 1; Figure 3). The WFPS values presented are calculated from the amount of water added during setup and are used only to compare treatments within the same soil. A non-significant decrease in WFPS by 4.5% (Luvisol I) and 8.9% (Luvisol II) due to the addition of 1% ASi compared to the control without ASi was found (Table 1; Figure 3). At 5% ASi addition, WFPS decreased significantly ( $p < 0.05$ ) by 21% (Luvisol I) and 26% (Luvisol II), whereas at 10% ASi addition, a significant ( $p < 0.05$ ) decrease by 83% (Luvisol I) and 81% (Luvisol II) compared to the controls were found. (Table 1; Figure 3).

In contrast to that, the addition of 1% ASi increased WFPS in both Arenosols, though only Arenosol II showed a significant increase by 15.9%, whereas Arenosol I showed a non-significant increase of 4.4% (Table 1; Figure 3). However, at 5% and 10% ASi, admixture, WFPS decreased in both Arenosols, similar to the studied Luvisols; however, this decrease was significant only at

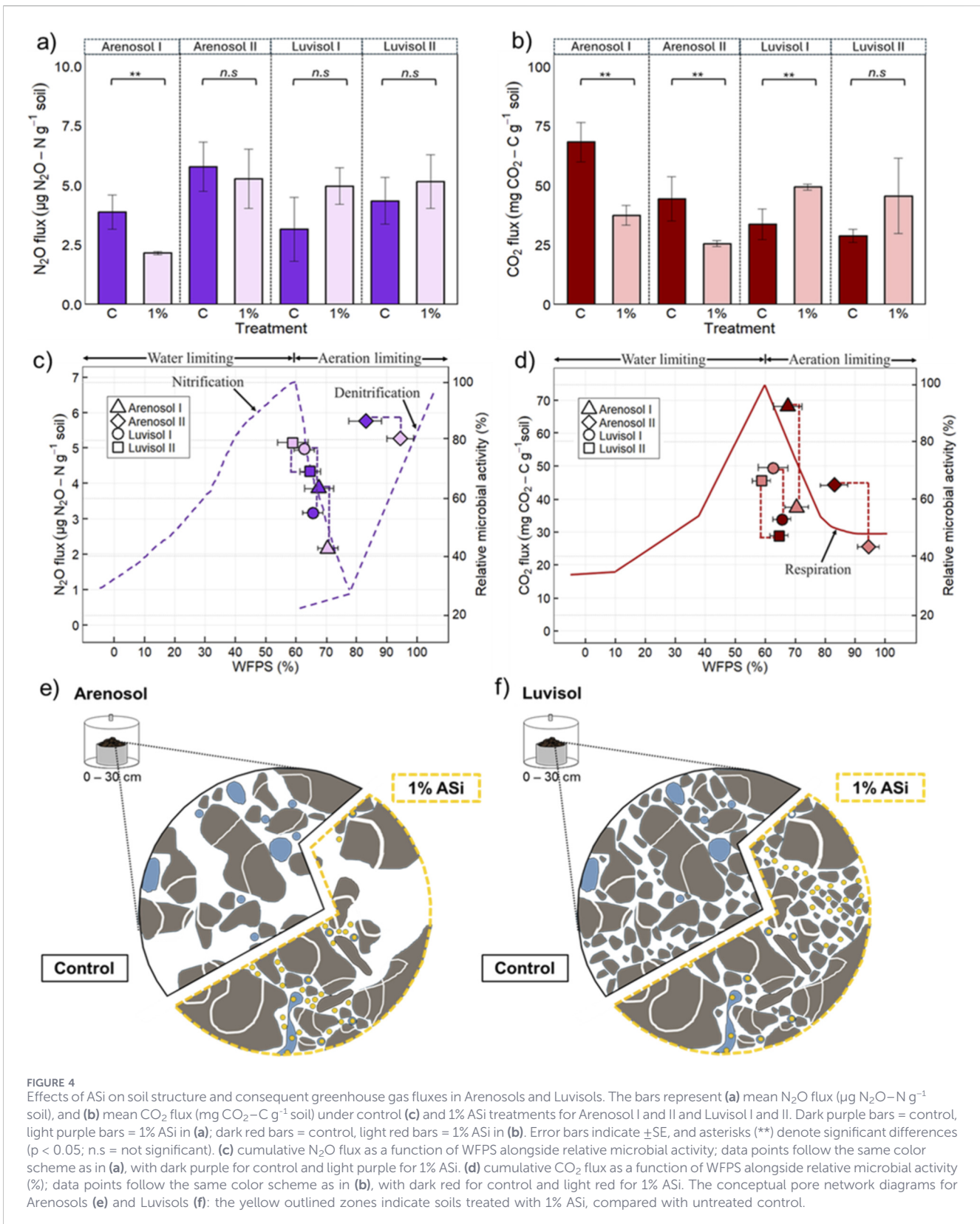


**FIGURE 4** Effects of ASI on soil structure and consequent greenhouse gas fluxes in Arenosols and Luvisols. The bars represent (a) mean N<sub>2</sub>O flux (μg N<sub>2</sub>O-N g<sup>-1</sup> soil), and (b) mean CO<sub>2</sub> flux (mg CO<sub>2</sub>-C g<sup>-1</sup> soil) under control (c) and 1% ASI treatments for Arenosol I and II and Luvisol I and II. Dark purple bars = control, light purple bars = 1% ASI in (a); dark red bars = control, light red bars = 1% ASI in (b). Error bars indicate ±SE, and asterisks (\*\*) denote significant differences (p < 0.05; n.s. = not significant). (c) cumulative N<sub>2</sub>O flux as a function of WFPS alongside relative microbial activity; data points follow the same color scheme as in (a), with dark purple for control and light purple for 1% ASI. (d) cumulative CO<sub>2</sub> flux as a function of WFPS alongside relative microbial activity (%); data points follow the same color scheme as in (b), with dark red for control and light red for 1% ASI. The conceptual pore network diagrams for Arenosols (e) and Luvisols (f): the yellow outlined zones indicate soils treated with 1% ASI, compared with untreated control.

10% ASI addition, with a reduction of 82% (Arenosol I) and 85% (Arenosol II) compared to the respective controls (Table 1; Figure 3). The low WFPS values observed at high ASI addition (e.g., ~11–12% at 10% ASI in Luvisols) reflect calculated values

derived from fixed water input and ASI-induced changes in bulk density, rather than directly measured soil moisture. These values therefore represent a relative index of pore water status and should not be interpreted as absolute moisture conditions. Thus, the

pronounced decrease in calculated WFPS mainly arises from increased total pore volume at constant water addition, rather than from an actual reduction in soil water content.

### 3.3 Effect of ASi addition on N<sub>2</sub>O and CO<sub>2</sub> emissions

We found clear trends in cumulative N<sub>2</sub>O (Figures 4a,c) and CO<sub>2</sub> (Figures 4b,d) emissions due to 1% ASi addition in both soil types during experiment II. These trends, however, varied with ASi addition in Arenosol, reducing and in Luvisol increasing the emissions; the direction and statistical significance of these responses differed between soils and gases. CO<sub>2</sub> responses were significant in Arenosols (and Luvisol I only), whereas N<sub>2</sub>O responses were not significant at several sampling locations (Table 1). Figures 4a,b show the mean N<sub>2</sub>O and CO<sub>2</sub> emissions for soil from the four sampling locations without and with the addition of 1% ASi. Across control treatments, Arenosols showed higher cumulative CO<sub>2</sub> emissions than Luvisols (Figure 4b), despite lower TOC (Table 1), indicating that baseline respiration differed between soil types under the standardized packing and water addition conditions. Figure 4c shows the cumulative N<sub>2</sub>O emission combined with the conceptual relationship between microbial activity and WFPS, whereas Figure 4d shows the corresponding CO<sub>2</sub> emission plotted against WFPS with the same conceptual curve (WFPS; 0%–100%) with and without 1% ASi. For consistency with Experiment I, WFPS values shown in Figures 4c,d are interpreted as a relative indicator under standardized water addition rather than as an absolute, directly comparable parameter across soils and treatments. The conceptual pore-network images (Figures 4e,f) provide a schematic illustration of how ASi amendment may influence pore structure. In these diagrams, the soil matrix is shown in grey, ASi particles in orange, and pore space in white. The diagrams are intended to illustrate inferred pore-scale changes consistent with the observed shifts in bulk density, calculated WFPS, and gas fluxes, rather than to represent directly measured pore-size distributions.

In Arenosols, N<sub>2</sub>O emissions decreased under 1% ASi treatment, coinciding with higher calculated WFPS relative to the control (Figures 4a,c). This decrease was significant in Arenosol I ( $p < 0.05$ ), where cumulative N<sub>2</sub>O emissions were reduced by 44.3%, while Arenosol II showed a non-significant ( $p > 0.05$ ) reduction by 8% compared to the respective controls (Table 1; Figures 4a,c). In contrast to Arenosols, Luvisol I and II showed a non-significant increase in N<sub>2</sub>O emissions of 57% and 18%, respectively, following 1% ASi addition, despite slightly lower calculated WFPS (Table 1; Figures 4a,c).

In the case of CO<sub>2</sub>, we found a significant ( $p < 0.05$ ) decrease in CO<sub>2</sub> emissions due to 1% ASi addition by 45% and 42% for Arenosol I and II, respectively (Table 1; Figures 4b,d), consistent with the direction of the calculated WFPS proxy observed in Experiment I under the same standardized water addition. In contrast, Luvisol I and II showed an increase in CO<sub>2</sub> emissions by 46.8%, which was only significant ( $p < 0.05$ ) in the case of Luvisol I, following 1% ASi addition, while the response in Luvisol II was not significant, despite only a slight decrease in WFPS (Table 1; Figures 4b,d).

## 4 Discussion

This study investigated how ASi addition can modify soil bulk density and the resulting WFPS proxy, and how these physical changes are associated with N<sub>2</sub>O and CO<sub>2</sub> emissions in soils with different silt contents. WFPS was calculated rather than measured continuously, and bulk density and WFPS in the incubation vessels were inferred from the standardized packing and water addition procedures based on responses quantified in Experiment I. This approach provides a controlled mechanistic framework for interpreting gas-flux responses, but it does not capture potential variability in soil structure or moisture dynamics that may occur in the field. Consequently, while relative treatment differences are meaningful under controlled conditions, absolute values of bulk density, WFPS, and their direct influence on N<sub>2</sub>O and CO<sub>2</sub> emissions remain uncertain. Therefore, gas flux responses observed in Experiment II as a result of ASi addition are interpreted as a consistent mechanistic pattern seen in the bulk density and WFPS index responses from Experiment I under the same fixed water addition, rather than serving as direct evidence of the conditions within the vessels. For this reason, oxygen availability and its influence on gas flux are discussed as an inferred mechanism.

Findings from Experiment I support our hypothesis that ASi addition alters the soil WFPS through changes in soil bulk density, but the response depends on the initial soil texture and ASi dose (Table 1; Figure 3). Under standardized packing, the response and changes in soil bulk density at 1% ASi was small and texture specific, with Arenosols increasing and Luvisols decreasing in bulk density, thus the WFPS, whereas at higher ASi addition (5%–10%), the bulk density and WFPS response converged across soils, indicating that increasing ASi dose can shift the packing and the resulting WFPS proxy in a way that dominates initial textural differences (Table 1; Figure 3). Thus, the direction and magnitude of ASi-induced changes in WFPS via changes in bulk density are not uniform but depend on the soil's initial texture and underlying pore structure.

Against this background, we propose two contrasting effects through which ASi may alter bulk density and thus WFPS: (i) when added to finer-texture Luvisol soils, ASi may decrease bulk density due to its low density and its fine particle size that can shift the pore size distribution. These may have reduced the packing efficiency and increased the total pore volume of the soil under standardized compaction (Figure 4f), which under fixed water input would lower the fraction of pore space filled with water and thus lower the WFPS (ii) when added to coarse-textured Arenosol soils, ASi may have reduce macroporosity by clogging larger pores, thereby enhancing the bulk density and WFPS (Barbosa et al., 2024). Depending on the amount of added ASi and which of these effects dominates at a particular soil texture, adding ASi may either increase or decrease bulk density, thus affecting WFPS.

Additionally, texture analysis showed that ASi behaves like silt- and clay-sized particles, increasing the fine fraction while proportionally reducing sand content (Table 1). This shift towards finer textures may have reduced macroporosity in sandy Arenosol (Figure 4e), thereby increasing WFPS. A likely consequence of the increase in fine fraction in the coarse-texture soils is that water may be retained more readily at the applied water input because smaller pores hold water more strongly within the

large pores typical of sandy soils. In contrast, in the already finer-textured Luvisols, ASI slightly lowers WFPS, potentially due to changes in pore structure, such as improved pore volume (Figure 4f) that lowers WFPS under fixed water input. This difference suggests that in finer-textured soils, the ASI-induced changes are less about adding new fractions and more about changes in packing and pore space, such that the total volume can increase without increasing the fraction of pore space filled with water under same water input. Thus, ASI may influence not only the amount of pore space through bulk density, but also the balance between pores that mainly transmit water and pores that retain water, which may help explain why WFPS can increase in Arenosols but decrease in Luvisol under identical water input. These textural effects highlight that the direction of ASI's influence on bulk density and WFPS is texture-dependent and determined by how ASI modifies the internal pore network and the relative distribution of micro-, meso-, and macropores.

The resulting aeration shifts match the observed decrease (Arenosols) or increase (Luvisols) in CO<sub>2</sub> and N<sub>2</sub>O emissions observed during experiment II. We found that 1% ASI addition to Arenosols caused an increase in bulk density, while Luvisols showed a decrease. Neither the increase nor the decrease in bulk density at 1% ASI treatment was significant (Table 1). However, at increased ASI levels (10%), both Arenosols and Luvisols showed a significant reduction in both bulk density and WFPS, suggesting that higher ASI levels may have increased the proportion of finer pores or enhanced internal porosity within soil aggregates, leading to a decrease in bulk density and WFPS.

In our second hypothesis, we proposed that ASI-induced WFPS changes via bulk density alteration would affect N<sub>2</sub>O and CO<sub>2</sub> emission dynamics. In Experiment II, contrasting responses to N<sub>2</sub>O and CO<sub>2</sub> emissions in Arenosols and Luvisols following ASI treatment were found, partially confirming the second hypothesis. The variations can be attributed to differences in soil texture that influence how ASI alters pore structure and bulk density, subsequently modulating the WFPS and oxygen availability.

For example, the incorporation of ASI in Arenosols resulted in an increase in WFPS, from 67.5% to 70.4% in Arenosol I and from 82.2% to 94.5% in Arenosol II (Figures 4c,d). This rise in WFPS may be attributed to a reduction in mesopore and macropore volume due to ASI addition. These changes likely limit oxygen availability and diffusion within the soil, thereby inhibiting microbial respiration, essential oxygen-dependent pathways for CO<sub>2</sub> production, supporting the decrease in CO<sub>2</sub> emissions in Arenosol (Figures 4b,d). These findings are in line with established relationships, indicating that microbial activity and GHG emissions decrease at high WFPS in response to oxygen limitation (Linn and Doran, 1984; Butterbach-Bahl et al., 2013).

We showed that N<sub>2</sub>O emissions were highest at elevated WFPS (~80%) compared to those at lower WFPS (~60), irrespective of treatment (Figure 4c). An Earlier study by Linn and Doran (1984) identified this moisture range as one where oxygen limitation favors denitrification, leading to high N<sub>2</sub>O production. However, studies by Müller and Clough (2014), Wrage-Mönnig et al. (2018), and Schlüter et al. (2025) indicate that denitrification can already occur at around 60% WFPS even in sand or weakly aggregated soils. This suggests that both nitrification and denitrification likely occurred concurrently in our soils, with denitrification becoming increasingly

dominant as WFPS increases. Müller and Clough (2014), Wrage-Mönnig et al. (2018), and Schlüter et al. (2025) further showed through isotopic and microscale studies that changes in pore connectivity and microsite oxygen distribution, rather than bulk water content alone, regulate the balance between nitrification and denitrification. These findings provide a mechanistic understanding for our observations, suggesting that ASI-induced structural changes can influence microsite oxygen dynamics in a similar manner (Müller and Clough, 2014; Wrage-Mönnig et al., 2018). Consistent with microscale studies, showing that pore connectivity and oxygen heterogeneity, rather than bulk water content alone, regulate concurrent nitrification and denitrification (Müller and Clough, 2014; Wrage-Mönnig et al., 2018), the mechanism summarized in our conceptual diagram (Figure 2c), together with the observed flux patterns shown in Figures 4c,d, suggest that ASI-related structural changes may modify gas fluxes by altering microsite oxygen availability. Oxygen limitation within the aggregates, even at intermediate moisture levels (60% WFPS), can lead to overlapping nitrification and denitrification activity. Thus, the effect of ASI on pore structure could modify the extent of these micro-oxic zones, shifting the relative contribution of different N<sub>2</sub>O-producing pathways under varying oxygen conditions. However, as the incubation was conducted with disturbed, repacked soil, pore connectivity and aggregate structure may differ from intact field conditions; nevertheless, under fixed water input and standardized compaction, spatially variable oxygen conditions are likely, given that air and water-filled pores coexist.

The high N<sub>2</sub>O fluxes at elevated WFPS therefore, reflect enhanced denitrification, which generally produces more N<sub>2</sub>O than nitrification processes at lower moisture levels (Davidson et al., 2000). However, with ASI treatment, further increases in WFPS beyond ~80% (up to ~95%) were associated with a slight reduction in N<sub>2</sub>O emissions compared to the control (Figures 4a,c), even though emissions at these high WFPS remained greater than at lower WFPS. This pattern suggests that while denitrification was a key contributor to the high N<sub>2</sub>O flux at elevated WFPS, the more extreme oxygen-limited condition induced by ASI at >80% WFPS may have promoted more complete denitrification, thus reducing net N<sub>2</sub>O production toward dinitrogen (N<sub>2</sub>) production (Linn and Doran, 1984; Davidson and Verchot, 2000). This shift in WFPS might have played a significant role in substantially reducing overall N<sub>2</sub>O emissions found in Arenosols over time. This suggests that beyond a certain threshold, an increase in WFPS could limit oxygen-dependent microbial processes, thereby reducing both CO<sub>2</sub> and N<sub>2</sub>O emissions.

Maillet et al. (2025) reported that soils with lower meso- and macroporosity, associated with WFPS, showed higher N<sub>2</sub>O emissions. In our study, this pattern was not uniform: in Luvisol, at lower WFPS under ASI treatment coincided with higher N<sub>2</sub>O emission compared to the untreated control (Figures 4a,c), whereas in Arenosol, under higher WFPS, due to ASI likely clogging meso- and macropores, coincided with lower N<sub>2</sub>O emission. These results indicate that microsite oxygen dynamics, rather than total WFPS alone, govern N<sub>2</sub>O production, and that the same WFPS can yield different emission outcomes depending on soil texture and pore connectivity (Wrage-Mönnig et al., 2018; Schlüter et al., 2025).

In contrast, the addition of ASI to Luvisol soil resulted in a decrease in WFPS, from 65.7% to 62.7% in Luvisol I and from 64.6%

to 58.8% in Luvisol II (Figures 4a,c). This adjustment in WFPS moved the conditions closer to the optimal WFPS range (40%–60%) for microbial nitrification and aerobic respiration (Linn and Doran, 1984). While Linn and Doran (1984) showed that nitrification dominates under such conditions, Schlüter et al. (2025) demonstrate that small oxygen-deficient microsite zones can still develop even within well-aerated soils, allowing localized denitrification to occur concurrently with nitrification. Thus, in ASi-treated Luvisol, the lower WFPS likely improved aeration and oxygen diffusion, promoting aerobic microbial respiration, while maintaining conditions that permit limited denitrification and associated N<sub>2</sub>O formation from localized anoxic zones. Compared to the untreated controls, these changes could explain the slightly higher CO<sub>2</sub> emissions and marginal difference in N<sub>2</sub>O fluxes observed in Figures 4b,c. For Luvisols, no significant increase in N<sub>2</sub>O emissions was observed; the small sample size (n = 4) may have reduced statistical power; increasing the sample size could demonstrate differences, through increased sensitivity, however. While ASi may contribute to lower N<sub>2</sub>O emissions by altering bulk density and WFPS, improved plant nitrogen uptake (Hoffmann et al., 2025) could further reduce available mineral N for microbial nitrification and denitrification, being a potential way to make agriculture more sustainable (Schaller et al., 2025). Mineral N (N<sub>min</sub>) concentrations were more or less similar across treatments (Table 1), suggesting that differences in initial substrate availability are unlikely to be the primary driver of the contrasting N<sub>2</sub>O and CO<sub>2</sub> responses following ASi addition. This is consistent with the experimental setup, as soils were sampled at the end of the growing season and no additional mineral N was applied prior to incubation. Under these controlled conditions, texture- and dose-dependent changes in soil physical properties (bulk density, inferred pore connectivity, and calculated WFPS) therefore provide a more likely explanation for the observed gas-flux patterns than variation in mineral N availability.

## 5 Limitations

It is still not clear, however, what the observed effect of ASi on WFPS and associated N<sub>2</sub>O and CO<sub>2</sub> emissions would mean under field conditions. Several aspects of our incubation design limit direct extrapolation: soils were disturbed and repacked; incubation was conducted at constant temperature with fixed headspace flow; WFPS was calculated rather than measured continuously, and the use of standardized water addition and a single WHC reference to compare treatments. Moreover, Experiment II did not include plants, and therefore, root uptake and rhizosphere effects that can reshape the moisture and oxygen microsite were not present. Under field conditions, denitrification dynamics and the balance between N<sub>2</sub>O production and reduction may differ due to intact aggregates, variable organic matter availability, and transient wetting-drying and precipitation events. In addition, other ASi-induced processes, such as enhanced crop growth and improved N uptake, may dominate or counteract the mechanisms observed under controlled incubation conditions, thereby changing the N<sub>2</sub>O and CO<sub>2</sub> responses across texture and moisture regimes.

## 6 Conclusion

In conclusion, our study particularly highlights ASi's effect on soil bulk density and WFPS proxy, and these effects are associated with texture-dependent changes in N<sub>2</sub>O and CO<sub>2</sub> emissions by shifting towards or from optimal conditions for microbial respiration, nitrification, and denitrification under controlled incubation. In Experiment I, ASi effects on bulk density and WFPS were texture- and dose-dependent. In Experiment II, the contrasting N<sub>2</sub>O and CO<sub>2</sub> responses between soil types coincided with the direction of ASi-induced shifts in the calculated WFPS, supporting a texture-specific role of ASi in modulating aeration controls on gas fluxes under controlled incubation conditions. These results suggest that ASi may be promising for modifying aeration-related controls on gas fluxes in coarse sandy soils, while in finer-textured soils it could have opposite effects. Field effects will heavily depend on actual soil texture, water regime, and management, and direct field observations are required to assess whether these patterns hold under realistic conditions. Under our experimental conditions, the highest N<sub>2</sub>O emissions coincided with the highest WFPS (>80%), where oxygen limitation favored denitrification as the dominant pathway. However, considering that partial oxygen limitation and denitrification can already occur around 60% WFPS, especially in coarse-textured soils, ASi-induced changes in packing-related physical condition may influence N<sub>2</sub>O production not only under saturated but also under moderately moist conditions. These considerations highlight the need for field-based studies across contrasting textures and moisture regimes to test whether the texture-dependent mechanism due to ASi treatment under controlled incubation conditions translates to managed soils under realistic soil structure, fluctuating water availability, and plant-soil interaction. Future work should therefore include ASi amendment under (i) field trials across texture gradients with crops present and (ii) coupled assessment of plant responses, mineral N dynamics, and CO<sub>2</sub> and N<sub>2</sub>O fluxes.

## Data availability statement

The raw data supporting the conclusions of this article will be made available by the authors, without undue reservation.

## Author contributions

PU: Writing – review and editing, Formal Analysis, Visualization, Data curation, Investigation, Writing – original draft. MH: Writing – review and editing, Validation, Methodology, Visualization, Conceptualization. ML: Methodology, Writing – review and editing, Investigation. KG: Writing – review and editing, Visualization. KK: Funding acquisition, Writing – review and editing. JS: Writing – review and editing, Validation, Supervision, Conceptualization, Funding acquisition.

## Funding

The author(s) declared that financial support was received for this work and/or its publication. The overall project was funded by the Deutsche Forschungsgemeinschaft for funding (SCHA 1822/14-1 and

KA 1737/21-1). Funding for the infrastructure of the patchCROP experiment was provided by the Leibniz Centre for Agricultural Landscape Research (ZALF) and the German Research Foundation under Germany's Excellence Strategy (EXC-2070-390732324 – PhenoRob). KG acknowledges support from BMBF for the Junior Research Group SoilRob (Grant 031B1391).

## Acknowledgements

We thank Oscar Monzon for help with analysis and Björn Gustav Wang and Felix Erbe for help during soil sampling and map visualization.

## Conflict of interest

The author(s) declared that this work was conducted in the absence of any commercial or financial relationships that could be construed as a potential conflict of interest.

## References

- Barbosa, L. A. P., Stein, M., Gerke, H. H., and Schaller, J. (2024). Synergistic effects of organic carbon and silica in preserving structural stability of drying soils. *Sci. Rep.* 14, 8330. doi:10.1038/s41598-024-58916-9
- Belton, D. J., Deschaume, O., and Perry, C. C. (2012). An overview of the fundamentals of the chemistry of silica with relevance to biosilicification and technological advances. *FEBS Journal* 279, 1710–1720. doi:10.1111/j.1742-4658.2012.08531.x
- Beretta, A. N., Silbermann, A. V., Paladino, L., Torres, D., Bassahun, D., Musselli, R., et al. (2014). Soil texture analyses using a hydrometer: modification of the bouyoucos method. *Cienc. Investig. Agrar.* 41, 25–26. doi:10.4067/s0718-16202014000200013
- Bezerra, F. S., de Mello Prado, R., Teixeira, G. C. M., Alves, D. M. R., da Costa Berto, S. D., Gonçalves, W. J. F., et al. (2025). Response of sugarcane under water deficit to amorphous silica doses: biomass, C: N: p homeostasis, and nutritional efficiency. *Plant Soil*, 1–23. doi:10.1007/s11104-025-08040-y
- Butterbach-Bahl, K., Baggs, E. M., Dannenmann, M., Kiese, R., and Zechmeister-Boltenstern, S. (2013). Nitrous oxide emissions from soils: how well do we understand the processes and their controls? *Philos. Trans. R. Soc. Lond. B Biol. Sci.* 368, 20130122. doi:10.1098/rstb.2013.0122
- Davidson, E. A., and Verchot, L. V. (2000). Testing the Hole-in-the-Pipe model of nitric and nitrous oxide emissions from soils using the TRAGNET database. *Glob. Biogeochem. Cycles* 14, 1035–1043. doi:10.1029/1999gb001223
- Davidson, E. A., Keller, M., Erickson, H. E., Verchot, L. V., and Veldkamp, E. (2000). Testing a conceptual model of soil emissions of nitrous and nitric oxides: using two functions based on soil nitrogen availability and soil water content, the hole-in-the-pipe model characterizes a large fraction of the observed variation of nitric oxide and nitrous oxide emissions from soils. *Bioscience* 50, 667–680. doi:10.1641/0006-3568(2000)050[0667:tacmos]2.0.co;2
- Engels, A. M., Gaiser, T., Ewert, F., Grahmann, K., and Hernández-Ochoa, I. (2025). Simulating soil moisture dynamics in a diversified cropping system under heterogeneous soil conditions. *Agronomy* 15, 407. doi:10.3390/agronomy15020407
- Evonik-Industries (2018). *Aerosil - Fumed silica technical overview*.
- Galindo, F. S., Pagliari, P. H., Rodrigues, W. L., Fernandes, G. C., Boleta, E. H. M., Santini, J. M. K., et al. (2021). Silicon amendment enhances agronomic efficiency of nitrogen fertilization in maize and wheat crops under tropical conditions. *Plants* 10, 1329. doi:10.3390/plants10071329
- Grahmann, K., Reckling, M., Hernández-Ochoa, I., Donat, M., Bellingrath-Kimura, S., and Ewert, F. (2024). Co-designing a landscape experiment to investigate diversified cropping systems. *Agric. Syst.* 217, 103950. doi:10.1016/j.agsy.2024.103950
- Guntzer, F., Keller, C., and Meunier, J.-D. (2012). Benefits of plant silicon for crops. *A Review. Agron. Sustainable Development* 32, 201–213. doi:10.1007/s13593-011-0039-8
- Hansen, L. V., Brændholt, A., Tariq, A., Jensen, L. S., Peixoto, L. E., Petersen, S. O., et al. (2024). Methane uptake rates across different soil types and agricultural management practices in Denmark. *Agric. Ecosyst. & Environ.* 363, 108878. doi:10.1016/j.agee.2023.108878
- Hoffmann, M., Jurisch, N., Borraz, E. A., Hagemann, U., Dröslér, M., Sommer, M., et al. (2015). Automated modeling of ecosystem CO<sub>2</sub> fluxes based on periodic closed chamber measurements: a standardized conceptual and practical approach. *Agric. For. Meteorology* 200, 30–45. doi:10.1016/j.agrformet.2014.09.005
- Hoffmann, M., Diaz, O. R. M., Zentgraf, I., Al-Hamwi, W., Dubbert, M., Stein, M., et al. (2025). Amorphous silica reduces N<sub>2</sub>O emissions from arable land at the field plot scale. *Front. Environ. Sci.* 13, 1522700. doi:10.3389/fenvs.2025.1522700
- Keeney, D. R., and Nelson, D. W. (1982). Methods of soil analysis: part 2 chemical and microbiological properties. *Nitrogen-inorganic forms* 9, 643–698.
- Linn, D. M., and Doran, J. W. (1984). Effect of water-filled pore-space on carbon-dioxide and nitrous-oxide production in tilled and nontilled soils. *Soil Sci. Soc. Am. J.* 48, 1267–1272. doi:10.2136/sssaj1984.03615995004800060013x
- Liu, J., Iskander, M. G., and Sadek, S. (2003). Consolidation and permeability of transparent amorphous silica. *Geotechnical Test. J.* 26, 390–401. doi:10.1520/gtj11257j
- Livingston, G., and Hutchinson, G. (1995). Enclosure-based measurement of trace gas exchange: applications and sources of error. *Biogenic Trace Gases: Measuring Emissions from Soil and Water*, 51, 14–51.
- Ma, J. F., and Yamaji, N. (2006). Silicon uptake and accumulation in higher plants. *Trends Plant Science* 11, 392–397. doi:10.1016/j.tplants.2006.06.007
- Madegwa, Y. M., Hu, Y., Schaller, J., and Butterbach-Bahl, K. (2025). Silicon fertilizer increased potato drought tolerance and reduced soil N<sub>2</sub>O emissions in two Danish soils at field scale. *Sci. Rep.* 15, 36111. doi:10.1038/s41598-025-24063-y
- Maillet, E., Grosse, A., Cousin, I., Arbaret, L., Cottenot, L., and Lacoste, M. (2025). What is the most relevant soil structure parameter to describe field-measured N<sub>2</sub>O emissions? *Geoderma* 453, 117155. doi:10.1016/j.geoderma.2024.117155
- Martos-García, I., Fernandez-Escobar, R., and Benlloch-González, M. (2025). Silicon affects growth and nitrogen uptake of young olive plants. *HortScience* 60, 1–4. doi:10.21273/hortsci.18259-24
- Mengel, K., and Kirkby, E. A. (1987). *Principles of plant nutrition*. International Potash Institute, 687.
- Müller, C., and Clough, T. (2014). Advances in understanding nitrogen flows and transformations: gaps and research pathways. *J. Agric. Sci.* 152, 34–44. doi:10.1017/s0021859613000610
- Pati, S., Pal, B., Badole, S., Hazra, G. C., and Mandal, B. (2016). Effect of silicon fertilization on growth, yield, and nutrient uptake of rice. *Commun. Soil Science Plant Analysis* 47, 284–290. doi:10.1080/00103624.2015.1122797
- R Core Team (2013). *R: a language and environment for statistical computing*. Vienna, Austria: R Foundation for Statistical Computing. Available online at: <http://www.R-project.org/>.
- Rea, R. S., Islam, M. R., Rahman, M. M., Nath, B., and Mix, K. (2022). Growth, nutrient accumulation, and drought tolerance in crop plants with silicon application: a review. *Sustainability* 14, 4525. doi:10.3390/su14084525

## Generative AI statement

The author(s) declared that generative AI was not used in the creation of this manuscript.

Any alternative text (alt text) provided alongside figures in this article has been generated by Frontiers with the support of artificial intelligence and reasonable efforts have been made to ensure accuracy, including review by the authors wherever possible. If you identify any issues, please contact us.

## Publisher's note

All claims expressed in this article are solely those of the authors and do not necessarily represent those of their affiliated organizations, or those of the publisher, the editors and the reviewers. Any product that may be evaluated in this article, or claim that may be made by its manufacturer, is not guaranteed or endorsed by the publisher.

- Rillig, M. C., Hoffmann, M., Lehmann, A., Liang, Y., Lück, M., and Augustin, J. (2021). Microplastic fibers affect dynamics and intensity of CO<sub>2</sub> and N<sub>2</sub>O fluxes from soil differently. *Microplastics Nanoplastics* 1, 1–11. doi:10.1186/s43591-021-00004-0
- Sagona, W. C. J., Kachala, O., Matete, S., and Jenya, H. (2016). Physiochemical properties of soil in selected sites of the Lake Chilwa basin after 5 years of conservation agriculture practice. *Univers. J. Agric. Res.* 4, 155–164. doi:10.13189/ujar.2016.040407
- Schaller, J., Cramer, A., Carminati, A., and Zarebanadkouki, M. (2020). Biogenic amorphous silica as main driver for plant available water in soils. *Sci. Rep.* 10, 2424. doi:10.1038/s41598-020-59437-x
- Schaller, J., Puppe, D., Kaczorek, D., Ellerbrock, R., and Sommer, M. (2021). Silicon cycling in soils revisited. *Plants (Basel)* 10, 295. doi:10.3390/plants10020295
- Schaller, J., Kleber, M., Puppe, D., Stein, M., Sommer, M., and Rillig, M. C. (2025). The importance of reactive silica for maintaining soil health. *Plant Soil* 513, 1–12. doi:10.1007/s11104-025-07299-5
- Schlüter, S., Lucas, M., Grosz, B., Ippisch, O., Zawallich, J., He, H., et al. (2025). The anaerobic soil volume as a controlling factor of denitrification: a review. *Biol. Fertil. Soils* 61, 343–365. doi:10.1007/s00374-024-01819-8
- Struyf, E., Smis, A., Van Damme, S., Garnier, J., Govers, G., Van Wesemael, B., et al. (2010). Historical land use change has lowered terrestrial silica mobilization. *Nat. Commun.* 1, 129. doi:10.1038/ncomms1128
- Weatherburn, M. (1967). Phenol-hypochlorite reaction for determination of ammonia. *Anal. Chemistry* 39, 971–974. doi:10.1021/ac60252a045
- Wedepohl, K. H. (1995). The composition of the Continental crust. *Geochimica cosmochimica Acta* 59, 1217–1232. doi:10.1016/0016-7037(95)00038-2
- Wrage-Mönnig, N., Horn, M. A., Well, R., Müller, C., Velthof, G., and Oenema, O. (2018). The role of nitrifier denitrification in the production of nitrous oxide revisited. *Soil Biol. Biochem.* 123, A3–A16. doi:10.1016/j.soilbio.2018.03.020
- Wu, D., Cárdenas, L. M., Calvet, S., Brüggemann, N., Loick, N., Liu, S., et al. (2017). The effect of nitrification inhibitor on N<sub>2</sub>O, NO and N<sub>2</sub> emissions under different soil moisture levels in a permanent grassland soil. *Soil Biol. Biochem.* 113, 153–160. doi:10.1016/j.soilbio.2017.06.007
- Zarebanadkouki, M., Hosseini, B., Gerke, H. H., and Schaller, J. (2022). Amorphous silica amendment to improve sandy soils' hydraulic properties for sustained plant root access under drying conditions. *Front. Environ. Sci.* 10, 935012. doi:10.3389/fenvs.2022.935012
- Zarebanadkouki, M., Al Hamwi, W., Abdalla, M., Rahnemaie, R., and Schaller, J. (2024). The effect of amorphous silica on soil-plant-water relations in soils with contrasting textures. *Sci. Rep.* 14, 10277. doi:10.1038/s41598-024-60947-1